Dissolved and Labile Particulate Zr, Hf, Nb, Ta, Mo and W in the Western North Pacific Ocean

M. Lutfi Firdaus*, Kazuhiro Norisuye, Yusuke Nakagawa, Seiji Nakatsuka and Yoshiki Sohrin

Institute for Chemical Research, Kyoto University, Uji, Kyoto 611-0011, Japan

Dissolved and labile particulate Zr, Hf, Nb, Ta, Mo and W were determined at stations K1 (51°N, 165°E), K2 (47°N, 160°E), KNOT (44°N, 155°E) and 35N (35°N, 160°E) in the western North Pacific Ocean. A portion of seawater for dissolved species (D) was passed through a 0.2 μm Nuclepore filter and acidified to pH 2.2 with HCl and HF. A portion of seawater for acid-dissolvable species (AD) was acidified without filtration. Labile particulate (LP) species is defined as AD minus D, which represents a chemically labile fraction of particulate species. D-Zr, Hf and Ta increase with depth, Nb shows a slight depletion in surface water, whereas Mo and W have a conservative vertical profile. The concentration range of D-Zr, Hf, Nb, Ta and W is 31–275, 0.14–0.95, 4.0–7.2, 0.08–0.29 and 40–51 pmol kg^{-1}, respectively, whereas that of Mo is 97–105 nmol kg^{-1}. LP-species of Zr, Hf and Ta account for 10–14% of AD in average and increase up to 25% below 4000 m, whereas those for Mo and W are negligible. In contrast, LP-Nb shows maxima (up to 27%) in surface water. We also found that D-Zr/Hf, Nb/Ta and Mo/W mole ratios generally increase in the order continental crust < river water < coastal sea < open ocean.

1. Introduction

Zr, Hf, Nb, Ta, Mo and W are adjacent metals in the periodic table, known as "high field strength elements" (HFSE) (Rudnick and Gao, 2005), and are of great interest in geochemistry. During the fractional crystallization of magma or magma generation by the partial melting of mantle, HFSE cannot easily enter cation sites of the minerals and concentrate in the magma (liquid phase). Because of their close chemical similarities (e.g. ionic charge and ionic radius), the ratios of Zr to Hf, Nb to Ta and Mo to W show limited variations in crustal materials (Jochum *et al.*, 1986; Li, 2000). The average mole ratio in the bulk continental crust is estimated to be 69 for Zr/Hf, 22 for Nb/Ta and 1.6 for Mo/W (Rudnick and Gao, 2005).

In seawater, Zr, Hf, Nb and Ta are classified as "refractory metals" (Orians and Merrin, 2001) and are dominated by hydroxide species (Turner *et al.*, 1981). They are not readily dissolved in seawater. Their supply to the ocean is low relative to their abundance in the crust. They are rapidly removed from solution by interaction with the

surfaces of sinking particles, a process referred to as "scavenging". Both of these factors result in very low concentrations in seawater. Thus, these metals are thought to have a potential use as an oceanographic tracer (McKelvey and Orians, 1998). Mo and W are dominated by oxyacid species, and are more soluble than hydroxide species (Turner *et al.*, 1981). Some papers on their oceanic distributions have been published. Boswell and Elderfield (1988) were the first to report the D-Zr and Hf concentrations in open ocean seawater, in addition to that in river and coastal water. They found that D-Zr in surface and deep water of the Indian Ocean was 80 and 185 pmol kg^{-1}, respectively, whereas it was 200 pmol kg^{-1} in the Atlantic deep water. They reported that D-Hf was 19–22 pmol kg^{-1}. McKelvey and Orians (1993) reported the first vertical profile of D-Zr in the ocean from the central North Pacific. They found that D-Zr ranged from 12–95 pmol kg^{-1} in surface water to a maximum of 300 pmol kg^{-1} in deep water. Godfrey *et al.* (1996) reported that the concentration of D-Zr and Hf in the northeastern Atlantic Ocean was in the range 70–180 pmol kg^{-1} and 0.4–1.1 pmol kg^{-1}, respectively. They stated that the distributions with depth indicate a nutrient-like scavenging-regeneration behavior, although the dissimilarity with silicate and nitrate in samples below the nutricline suggest

---

that other mechanisms are also important in defining the oceanic distribution of Zr and Hf. McKelvey and Orians (1998) reported concentrations of D-Zr and Hf at station P26 (55°N, 145°W) in the subarctic North Pacific of 25–366 pmol kg^{-1} and 0.20–1.02 pmol kg^{-1}, respectively. Collier (1985) analyzed D-Mo in the Northeast Pacific Ocean and concluded that D-Mo concentration was 107 nmol kg^{-1} on average and its distribution is not significantly affected by biological cycling. Our group found that D-Mo and W had uniform profiles in the North Pacific Ocean and their concentrations normalized to S = 35 were 104–106 nmol kg^{-1} and 53–60 pmol kg^{-1}, respectively (Sohrin *et al.*, 1987, 1999). Our group also reported the vertical profiles of D-Zr, Hf, Nb, Ta, Mo and W in the western North Pacific (Sohrin *et al.*, 1998). D-Zr and Hf were in the range 30–250 and 0.10–0.85 pmol kg^{-1}, respectively. The mean concentrations of D-Nb in surface and deep water were 3.0 and 3.8 pmol kg^{-1}, respectively, and those of D-Ta were 0.08 and 0.20 pmol kg^{-1}. D-Nb showed a slight depletion in surface water and D-Ta showed a slight increase near the bottom. All samples in these previous reports were filtered through a filter with a pore size of 0.45 or 0.2 μm, and therefore the concentrations are those of dissolved species.

Recently, we have developed a new analytical method to determine these metals in seawater (Firdaus *et al.*, 2007). The method was applied to the seawater samples taken from the western North Pacific Ocean. A portion of seawater for D species was passed through a 0.2 μm filter and acidified to pH 2.2 with HCl and HF. A portion of seawater for acid-dissolvable (AD) species was acidified without filtration. AD metals consist of the dissolved fraction and the labile particulate (LP) fraction that was dissolved during storage. The latter fraction would contain species such as those adsorbed on clay minerals, iron oxyhydroxide and manganese oxide, and those incorporated in organisms (Ezoe *et al.*, 2004). Here, we present for the first time the full depth-profiles of Zr, Hf, Nb, Ta, Mo and W in the form of D and LP species in the western North Pacific Ocean. We also analyzed various hydrospheric samples such as river and rain water. Therefore, together with seawater, we provide a more comprehensive discussion of the distributions of these six metals in the hydrosphere.

2. Materials and Methods

The detailed analytical method has been published elsewhere (Firdaus *et al.*, 2007).

2.1 Chemicals

Ultra-high purity CH$_3$COOH, NH$_3$ (Tamapure AA-100, Tama Chemicals, Japan), HF and HNO$_3$ (Ultrapur-100, Kanto Chemical, Japan) were used for the analysis of seawater. Metal standard solutions (1,000 mg L^{-1}) were
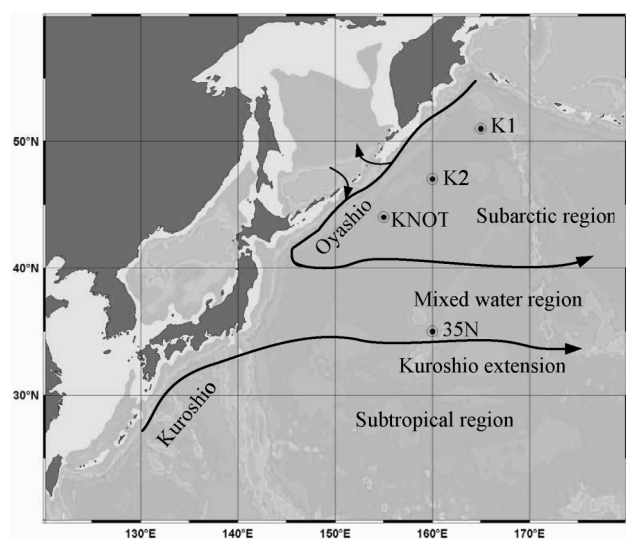

Fig. 1. Sampling location.

obtained from Wako Pure Chemical, Japan. Working standards in the range of pmol kg^{-1}–nmol kg^{-1} were prepared in a low-density polyethylene (LDPE) bottles (Nalge Nunc Int., USA) by dilution on a weight basis. Ultra pure water prepared with a Milli-Q water system (Gradient A-10, Millipore, USA) and was used to prepare all solutions. This is referred to as Milli-Q water hereafter.

2.2 Samples

Seawater samples were collected from four stations (Fig. 1) during the MR05-01 cruise of R/V Mirai (JAMSTEC) on March 2005 using a CTD carousel, on which Niskin-X samplers were mounted. The interior of the samplers was coated with Teflon and cleaned with detergent and HCl. Seawater was transferred from the sampler to LDPE bottles on deck using a silicon tube and filling bell to avoid contamination by airborne particles. Samples were immediately brought into a clean room laboratory (class 100) on the vessel. A portion of seawater for the D species was passed through a 0.2 μm Nuclepore filter (Costar, USA) using a closed filtration system and acidified to pH 2.2 with HCl and HF. A portion of seawater for the AD species was acidified without filtration. These samples were stored at ambient temperature for 7 months until analysis. Only D species were determined in the samples from station KNOT.

We also determined the metal concentrations of D species in several hydrospheric samples. Rainwater was collected on the roof of a 5-story building at the Uji Campus, Kyoto University. Rain water 1 was collected in the first week of November 2006. Rain water 2 and 3 were collected in the third and fourth week of December 2006,

respectively. The Uji River water was collected near the Uji Campus in the first week of October 2006. SLRS-3 is a river water reference material for trace metals (National Research Council Canada), which is derived from the Ottawa River, Canada. CASS-3 is a near-shore seawater reference material for trace metals (National Research Council Canada), which is derived from the Halifax Harbor, Canada. The concentrations of Zr, Hf, Nb, Ta, Mo and W have not previously been reported for both SLRS-3 and CASS-3.

2.3 Procedure for preconcentration and determination

A closed preconcentration system with a TSK-8-hydroxyquinoline resin (TSK-8HQ) column was used to preconcentrate the analytes. Prior to use, the column was washed by flushing with 20 mL of 5 M HF. Diluted $CH_3COOH-NH_3$ buffer (10 mL, 10^{-3} M, pH 5.2) was passed through to condition the pH in the column. The sample solution was buffered with 10^{-3} M $CH_3COOH-NH_3$ to pH 5.2 and then passed through the column, followed by 10 mL of the diluted $CH_3COOH-NH_3$ buffer to remove the sea salts remaining in the column. Finally, the adsorbed metals were eluted by back flushing with 20 mL of 5 M HF. The eluate was evaporated to dryness using a closed evaporation system. The metals were then re-dissolved in 5 mL of 0.5 M HNO_3 and made ready for determination.

Concentrations of Zr, Hf, Nb, Ta and W in the solution were determined by ICP-MS (Elan DRC II, Perkin Elmer). Observed isotopes were ^{90}Zr, ^{91}Zr, ^{177}Hf, ^{178}Hf, ^{93}Nb, ^{181}Ta, ^{182}W and ^{183}W. Mo concentration was determined by ICP-AES (Optima 2000 DV, Perkin Elmer), using emission lines at 202.034 and 203.848 nm. The procedure blank determined using Milli-Q water as a sample were 0.35, 0.009, 0.19, 0.005 and 0.37 pmol kg^{-1} for Zr, Hf, Nb, Ta and W, respectively, whereas that for Mo was 0.92 nmol kg^{-1}. Precisions were 2–4% for all the metals.

3. Results

3.1 Hydrography

Data on temperature and salinity together with the dissolved and acid-dissolvable trace metals are summarized in Appendix. Figure 1 shows that the three northern stations were located in the Western Subarctic Gyre (WSG), whereas station 35N (35°N, 160°E) was located at the southern edge of the Mixed Water Region (Qiu, 2001; Tatebe and Yasuda, 2004). A T-S diagram (Fig. 2) indicates that the Pacific Deep Water (PDW; T = 1.4–1.9°C, S = 34.56–34.69) occupied deep water (>2,000 m) at all stations. In the northern three stations (K1, K2 and KNOT), surface water was dominated by the Pacific Subarctic Upper Water (PSUW; T = 1.4–2.3°C, S = 33.16–33.23; Emery, 2001). Surface water of the lowest latitude
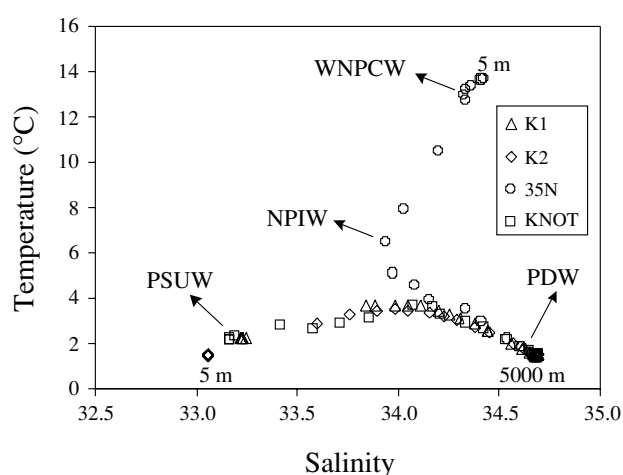

Fig. 2. T-S diagram. Abbreviations are Pacific Deep Water (PDW), North Pacific Intermediate Water (NPIW), Western North Pacific Central Water (WNPCW) and Pacific Subarctic Upper Water (PSUW).

station (35N) was strongly affected by the Western North Pacific Central Water (WNPCW; T = 12.7–13.7°C, S = 34.32–34.42). The salinity minimum at depths from 250 to 400 m of station 35N was characterized as the North Pacific Intermediate Water (NPIW; T = 5.1–7.9°C, S = 33.97–34.02).

3.2 Vertical profiles of D and LP trace metals

Figures 3 and 4 show vertical profiles of D and LP-Zr, Hf, Nb, Ta, Mo and W at stations K1 and 35N, respectively. The vertical profiles at stations K2 and KNOT are similar to those at station K1. D-Zr, Hf and Ta show an increase with depth. D-Nb shows a slight depletion in surface water and a slight enrichment in bottom water. The lowest concentrations of Zr, Hf, Nb and Ta in surface water are found at station 35N, which is the most pelagic among the four stations. The distribution of D-Mo and W are uniform both vertically and horizontally. The concentration is 100 ± 3 nmol kg^{-1} for Mo and 46 ± 3 pmol kg^{-1} for W (n = 94).

Previously, we reported the vertical profiles of these metals at station A (45°N, 164°E; Sohrin et al., 1998), which is close to stations K1 and K2. D-Nb at station K1 is 1 to 3 pmol kg^{-1} higher than that at station A. D-Ta at station K1 is also higher in the upper water column in comparison with that at station A. This is probably because the previous eluent of 0.5 M nitric acid containing 10^{-2} M oxalic acid resulted in a lower recovery of Nb and Ta than the 5 M HF that we used as eluent in this study. Moreover, our D-Zr, Hf, Mo and W data are oceanographically consistent with the previous studies (Collier, 1985; Sohrin et al., 1987, 1999; Godfrey et al.,
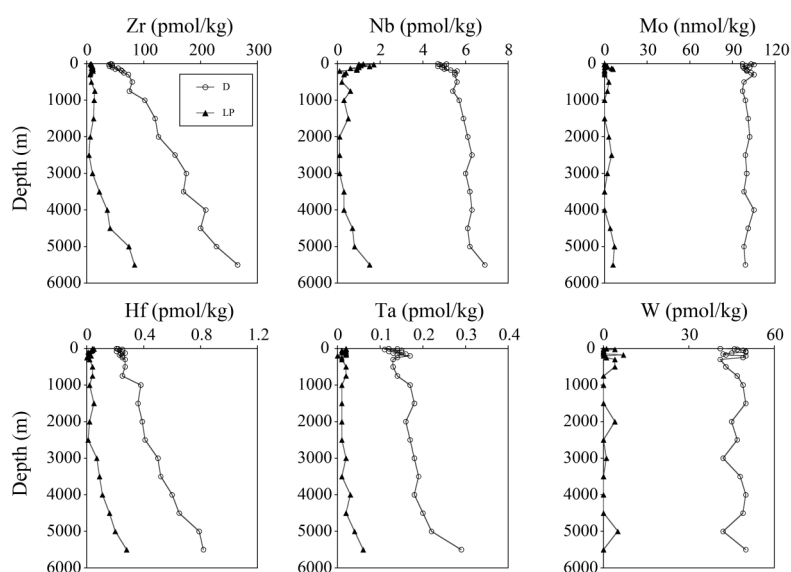
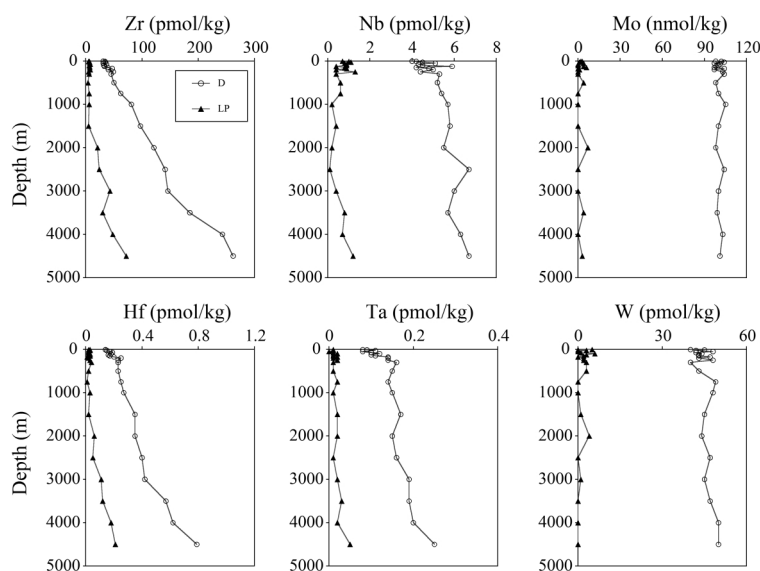Fig. 3. Vertical profiles of D and LP-metals at station K1.

Fig. 4. Vertical profiles of D and LP-metals at station 35N.

1996; McKelvey and Orians, 1998).

LP-Zr and Hf are nearly constant from surface to 3,000–3,500 m depths at stations K1 and K2, and increase to the bottom. The increase starts at a 1,500 m depth at station 35N. LP-Nb is enriched in both surface and bottom water. The surface maximum is more prominent in WSG. LP-Ta is almost constant from the surface to 3,000–4,500 m depths and shows enrichment in bottom water. LP-Mo and W have a uniform profile throughout the water column.

Compared to the AD species at the same depth, LP-Zr ranges from 3% at mid-depth to 24% in bottom water. LP-Hf ranges from less than 2% in surface water to 25% in bottom water. LP-Nb ranges from less than 1% at mid-depth to 27% in surface water, while LP-Ta ranges from less than 4% at shallow and mid-depths to 19% above the bottom. On the basis of data from the three stations, the percentage of LP is 1.7 ± 2.2 for Mo and 3.4 ± 4.2 for W ($n = 70$). These values suggest that the LP species are negligible for Mo and W.

Table 1. Metal concentrations in various hydrospheric samples.

Samples	Zr	Hf	Nb	Ta	Mo	W	Notes
					(pmol kg^{-1})		
Rain water							
1	41	0.36	4.5	0.26	349	12	This study
2	114	0.91	2.5	0.11	3.1×10^3	38	This study
3	124	1.2	5.1	0.24	2.3×10^3	23	This study
River							
Uji	453	3.6	75	3.8	4.4×10^3	171	This study
SLRS-3	678	4.9	31	1.4	2.1×10^3	22	This study
Arita	—	—	—	—	2.8×10^3	33	Sohrin *et al.* (1989)
Yodo	—	—	—	—	2.0×10^3	26	Sohrin *et al.* (1989)
Apure	300	3.2	—	—	—	—	Godfrey *et al.* (1996)
Orinoco	320	3.5	—	—	—	—	Godfrey *et al.* (1996)
Skagafjordur	—	—	—	—	$210–4.1 \times 10^3$	$27–1 \times 10^3$	Arnorsson and Oskarsson (2007)
St. Lawrence	242	17.4	22.5	—	13.5×10^3	—	Gaillardet *et al.* (2005)
Amazon	297	—	—	—	1.82×10^3	—	Gaillardet *et al.* (2005)
World average	429	33.1	18.2	6	4.38×10^3	543	Gaillardet *et al.* (2005)
Coastal seawater							
CASS-3	90	0.49	6.7	0.21	8.5×10^4	43	This study
NASS-5	183	1.24	7.8	0.25	—	37	Firdaus *et al.* (2007)

3.3 Hydrospheric samples

Table 1 summarizes the D metal concentrations in various hydrospheric samples, together with some literature data. There are 2.0–3.3 fold variations in the concentrations of Zr, Hf, Nb, Ta, and W among the three different rain samples. Mo shows a larger variation (8.9 fold).

The concentrations of Zr and Hf in the Uji and Ottawa Rivers agree well with the literature data. However, our Hf concentrations are one order lower than the world average. Reports of Nb and Ta data for river water are scarce. Our data seem to be consistent at least with the available data. The Mo concentrations in the Uji and Ottawa Rivers agree well with the literature data, except for the high concentration in the St. Lawrence River. W in river water shows much larger variations than Mo. W concentration reached 3.3×10^3 pmol kg^{-1} at the Yodo River estuary, which is located in an industrial metropolis, Osaka City. Arnorsson and Oskarsson (2007) found that the W concentrations in river and stream water in the Tertiary tholeiites area in Iceland lie in the range of 27 pmol kg^{-1}–1 nmol kg^{-1}.

In the Atlantic coastal seawater, CASS-3 and NASS-5, the concentrations of Zr, Hf and Ta are high compared with those in Pacific surface waters.

4. Discussions

4.1 Elemental fractionation in the hydrosphere

Figure 5 shows the dissolved mole ratio of various hydrospheric samples, where the ratio of continental crust and sediment (pelagic clay) is plotted together as a dotted and broken line, respectively. Zr/Hf and Nb/Ta concentrations in rain water show slightly higher ratios than the crustal ratio, whereas that of Mo/W is substantially higher than the crustal ratio. Therefore, it is obvious that the rain water samples are highly enriched in Mo, probably due to anthropogenic sources. Uji City, where the rain water samples were collected, is one of the industrial cities in the southern Kyoto area. Industrial and vehicular activities probably form the main source of Mo detected in the rain water samples. Mo is used as an alloying metal in steels, cast irons, and super alloys. A significant amount of Mo is used in catalyst preparation (Park *et al.*, 2006). Molybdenum sulfide is added to gasoline as a lubricant. Our group reported the concentrations of W in rain water collected in Otsu City, which is contiguous with Uji City (Mito *et al.*, 2004). The W concentrations varied from 9.5 to 2.2×10^3 pmol kg^{-1}. Thus, it is likely that W in these rain water samples is also affected by anthropogenic contamination.
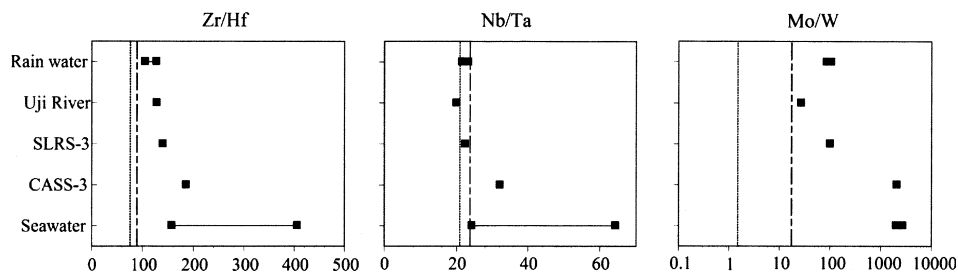
Fig. 5. D mole ratios in various hydrospheric samples. The dotted line shows the crustal ratio (data from Rudnick and Gao, 2005), the broken line shows the pelagic clay ratio (data from Li, 2000).
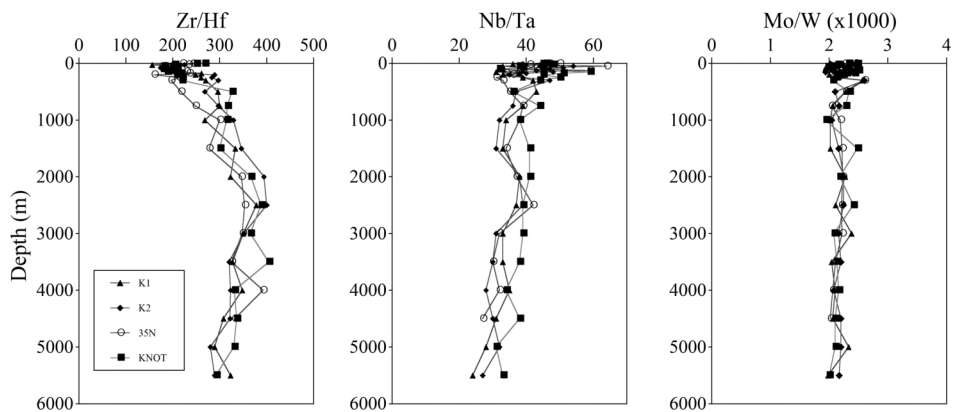

Fig. 6. D mole ratios in seawater.

The Zr/Hf, Nb/Ta and Mo/W mole ratios of the Uji River and SLRS-3 lay between the crustal and seawater ratios, except that the Nb/Ta ratio in the Uji River is slightly lower than the crustal ratio. The ratios of Zr/Hf, Nb/Ta and Mo/W generally increase in the order continental crust < river water < coastal sea < open ocean. The largest variation of Zr/Hf and Nb/Ta occurs in seawater, which reach to 3–5 fold higher values than the crustal ratios. The Mo/W ratio shows a small variation in seawater. However, the ratio in seawater is 2,000 times higher than the crustal ratio. Thus, the Mo/W pair shows much greater fractionation in the hydrosphere than that of Zr/Hf and Nb/Ta. Profiles of D-Zr/Hf, Nb/Ta and Mo/W mole ratios in the western North Pacific are shown in Fig. 6. The D-Mo/W ratio shows a uniform profile throughout the water column, with an average of 2,200 ± 160 (n = 94). Thus, it seems that D-Mo and W are hardly fractionated in the oxic ocean.

The D-Zr/Hf ratio increases with depth and becomes relatively constant in PDW (Fig. 6). The average Zr/Hf ratio from the surface to 200 m is 207 ± 25 (n = 36). At 250 to 500 m depths at station 35N, the Zr/Hf ratio is decoupled from that at the other three stations, with an average of 209 ± 12 (n = 3). The decoupled Zr/Hf ratio at station 35N should be a signature of NPIW, which passes through this station at depths of 250–400 m. The ratio at the same depths for stations K1, K2 and KNOT is 271 ± 35 (n = 9). The average ratio in PDW is 341 ± 34 (n = 30). These results suggest that the difference in the Zr/Hf ratio is probably due to different water masses. The potential usage of D-Zr/Hf elemental ratios as water masses tracer is also revealed in the plot of D-Zr/Hf to Sigma-θ (Fig. 7). Each water mass has a unique set of D-Zr/Hf and Sigma-θ. The four different water masses are clearly identified in Fig. 7.

Our D-Zr/Hf profile is similar to that reported for a station in the eastern North Pacific (55°N, 145°W; Orians and Merrin, 2001). Godfrey et al. (1996) reported that the D-Zr/Hf ratio in the northeastern Atlantic varies between 164 and 250. These data imply that the Zr/Hf ratio increases with deep water circulation. D-Zr is enriched in PDW compared to NADW. By contrast, the concentrations of D-Hf are relatively constant between the Atlantic and Pacific, which is similar to the case of D-Fe (Johnson et al., 1997). This could be attributable to the fact that D-Hf is more intensively scavenged in deep water
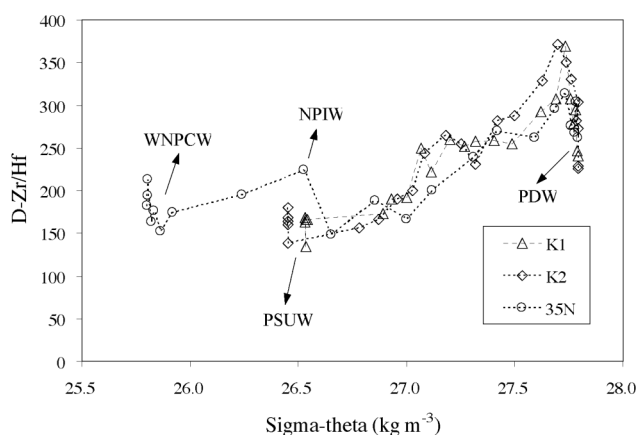
252   M. L. Firdaus *et al.*
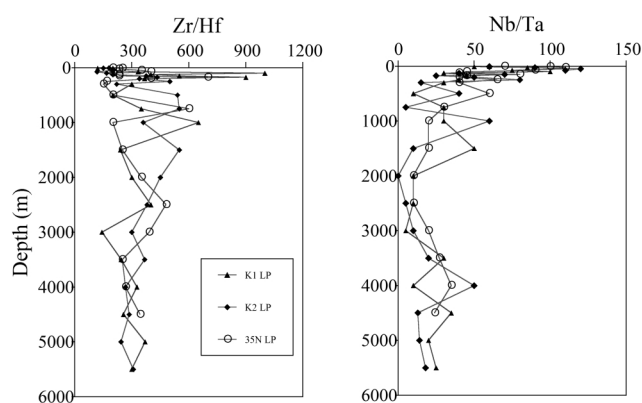
Fig. 7. Plot of D-Zr/Hf to Sigma-θ.

Fig. 8. LP mole ratios in seawater.

than D-Zr. LP-Zr/Hf shows a larger variation in the upper water column, with peaks at 100–175 m depths (Fig. 8). The LP-Zr/Hf ratio is 319 ± 76 (*n* = 22) in PDW. Although this value is close to the D-Zr/Hf ratio, it is much higher than the Zr/Hf ratio of 91 in pelagic clay. These results suggest that LP-Zr and Hf originate from the scavenging of the dissolved species in deep water.

Conversely to Zr/Hf, the D-Nb/Ta mole ratio in surface water (0–200 m depths) is higher (with an average of 42 ± 7.2; *n* = 56) than that in PDW (33 ± 4.7; *n* = 30; Fig. 6). The LP-Nb/Ta ratio is high and variable in surface water, with a minimum of 9 ± 5.5 (*n* = 9) at 2,000–3,000 m depths and a maximum of 25 ± 11 (*n* = 13) in bottom water (3,500 m–bottom; Fig. 8). The LP-Nb/Ta value in bottom water is close to the Nb/Ta ratio of 24 in pelagic clay. Thus, it is probable that the mechanism controlling the LP mole ratio is different between Nb/Ta and Zr/Hf. D-Nb and Ta have an intermediate profile between a Zr type and a Mo type, suggesting weak scavenging. Thus, it is likely that the increase of LP-Nb and Ta in bottom water can mainly be attributed to re-suspension of sediment.

4.2 Residence time

For a well-stirred, steady-state ocean, residence time of a metal (τ) is defined as:

$$\tau = \left(\text{Mean concentration of the metal in the ocean} \times \text{Ocean volume}\right) / \text{Total input of the metal per year}.$$

Here we estimate τ of the dissolved species. τ is calculated based on two major inputs of the metals to the ocean: river and atmospheric inputs. Due to scarceness of data, we ignore other possible inputs, such as hydrothermal, submarine groundwater discharge and sediment fluxes.

The mean concentration in the well-stirred, steady-

state ocean is assumed to be [Zr] = 220 pmol kg^{-1}, [Hf] = 0.8 pmol kg^{-1}, [Nb] = 7.2 pmol kg^{-1}, [Ta] = 0.25 pmol kg^{-1}, [Mo] = 104 nmol kg^{-1} and [W] = 49 pmol kg^{-1}. The ocean volume is 1.35×10^{21} kg. Assuming annual river discharge of 3.74×10^{16} kg y^{-1}, an annual rain water input of 0.1 kg cm^{-2}y^{-1} with the oceanic area of 0.36×10^9 km^2 (Nozaki *et al.*, 1997), and using the data in Table 1 as a mean concentration in river and rain water, we obtain river fluxes of [Zr] = 2.5×10^{19} pmol y^{-1}, [Hf] = 1.8×10^{17} pmol y^{-1}, [Nb] = 1.2×10^{18} pmol y^{-1}, [Ta] = 5.0×10^{16} pmol y^{-1}, [Mo] = 7.6×10^{16} nmol y^{-1} and [W] = 7.9×10^{17} pmol y^{-1}. The atmospheric fluxes are [Zr] = 4.1×10^{19} pmol y^{-1}, [Hf] = 3.3×10^{17} pmol y^{-1}, [Nb] = 9.0×10^{17} pmol y^{-1}, [Ta] = 3.9×10^{16} pmol y^{-1}, [Mo] = 1.3×10^{20} pmol y^{-1} and [W] = 4.3×10^{18} pmol y^{-1}. We obtain τ of 4,700 y for Zr; 2,200 y for Hf; 4,600 y for Nb; 3,900 y for Ta; 740,000 y for Mo and 14,000 y for W. The τ calculation for Nb and Ta is the first to be reported. The τ for Zr and Hf agrees well with the previous calculations of 5,000–5,600 y for Zr and 1,300–1,500 y for Hf (Godfrey *et al.*, 1996; Sohrin *et al.*, 1998). The τ for Mo and W seems to be shorter than previous reports, which give 800,000 y for Mo and 61,000 y for W (Sohrin *et al.*, 1998; Morford and Emerson, 1999). This is probably due to pollution of Mo and W in the rain water samples that we obtained for this study.

4.3 Box model

D-Zr and Hf exhibit vertical profiles with surface depletion (Figs. 3 and 4), which closely resemble those for light rare earth elements (Nozaki, 2001). To describe the geochemical cycling of D-Zr and Hf in the ocean, such as removal from surface water by scavenging of particulate matter, a two-box, steady-state model is calculated here in accordance with the model for Y and Ho (Nozaki *et al.*, 1997). The change in concentration of Zr in the surface-ocean box with time is:

$$V_S \frac{d[\mathbf{Zr}]}{dt} = R_{\mathbf{Zr}} + E_{\mathbf{Zr}} + v[\mathbf{Zr}]_D - v[\mathbf{Zr}]_S - \gamma_{\mathbf{Zr}}[\mathbf{Zr}]_S V_S \quad (1)$$

where:

$R_{\mathbf{Zr}}$ = River flux of Zr
$E_{\mathbf{Zr}}$ = Atmospheric flux of Zr
v = Volume of water exchange between surface and deep ocean box
$[\mathbf{Zr}]_D$ = Concentration of Zr in the deep ocean box
$[\mathbf{Zr}]_S$ = Concentration of Zr in the surface ocean box
V_S = Volume of the surface reservoir
$\gamma_{\mathbf{Zr}}$ = First-order rate constant for removal of the surface Zr to the deep box in particulate form.

Similarly, for Hf we have:

$$V_S \frac{d[\mathbf{Hf}]}{dt} = R_{\mathbf{Hf}} + E_{\mathbf{Hf}} + v[\mathbf{Hf}]_D - v[\mathbf{Hf}]_S - \gamma_{\mathbf{Hf}}[\mathbf{Hf}]_S V_S$$
$$(2)$$

Assuming a steady-state ($d[\mathbf{X}]/dt = 0$) and combining Eqs. (1) and (2), we obtain:

$$P_{\mathbf{Zr/Hf}} = K_D \frac{[\mathbf{Zr}]_S}{[\mathbf{Hf}]_S}$$
$$= \frac{R_{Zr} + E_{Zr} + v_S([\mathbf{Zr}]_D - [\mathbf{Zr}]_S)}{R_{Hf} + E_{Hf} + v_S([\mathbf{Hf}]_D - [\mathbf{Hf}]_S)} \quad (3)$$

where:

$P_{\mathbf{Zr/Hf}}$ = Zr/Hf atomic ratio in the vertical particulate flux
$K_D = \gamma_{\mathbf{Zr}}/\gamma_{\mathbf{Hf}}$
  = Distribution coefficient (fractionation factor) during the removal of Zr and Hf particles.

Here we assume that D-Zr and Hf are supplied to the ocean as dissolved species in river and rain water. From Table 1, we have concentrations in river and rain water of $[Zr]_{River}$ = 678 pmol kg^{-1}, $[Zr]_{Rain}$ = 114 pmol kg^{-1}, $[Hf]_{River}$ = 4.9 pmol kg^{-1} and $[Hf]_{Rain}$ = 0.91 pmol kg^{-1}. Calculated in a similar manner as that given above (Subsection 4.2), we obtain R_{Zr} = 2.5 × 10^{19} pmol y^{-1}, R_{Hf} = 1.8 × 10^{17} pmol y^{-1}, $E_{\mathbf{Zr}}$ = 4.1 × 10^{19} pmol y^{-1} and $E_{\mathbf{Hf}}$ = 3.3 × 10^{17} pmol y^{-1}. Using our Zr and Hf data in the western North Pacific as a global average, we have $[Zr]_S$ = 53 pmol kg^{-1}, $[Zr]_D$ = 187 pmol kg^{-1}, $[Hf]_S$ = 0.23 pmol kg^{-1} and $[Hf]_D$ = 0.57 pmol kg^{-1}. Taking v = 2 × 10^{18} kg y^{-1} and V_S = 7.2 × 10^{19} kg, we found that the flux of Zr and Hf from deep water box is 26.8 × 10^{19} and 6.8 × 10^{17} pmol kg^{-1}, respectively. Finally, we found that K_D = 1.2. Thus, the first-order removal rate constant of Zr in surface water is 1.2 times higher than that of Hf. The rapid removal of Zr from surface water is balanced by the high flux of Zr from deep water (about 10 times higher than its river flux), which probably results from regeneration of scavenged Zr, and/or a deep water source of Zr, such as hydrothermal flux. This result is consistent with the low D-Zr/Hf mole ratio in surface water (Figs. 5 and 6).

5. Conclusions

Here we have demonstrated that different water masses can be traced using the D-Zr/Hf mole ratio. The water mass signatures of WNPCW, NPIW, PSUW and PDW were successfully identified in the western North Pacific Ocean. We found that the bottom enrichments of LP-Zr and Hf are due to scavenging, whereas those of Nb and Ta are due to re-suspension of sediment. LP-Mo and W concentrations are negligible.

Although the Zr/Hf, Nb/Ta and Mo/W ratios lies in a narrow range in most rocks, the ratios start to become fractionated when the metals are introduced into the hydrosphere. The Zr/Hf, Nb/Ta and Mo/W ratios generally increase in the order continental crust < river water < coastal sea < open ocean.

To gain a better understanding of the behavior of these metals in the ocean, the study should be continued, with an emphasis on several points, as follows: (1) Analyze total suspended particulate matter as compared with LP; (2) Observe the ocean sections and examine the horizontal distribution of these metals; (3) Evaluate the hydrothermal, submarine groundwater discharge and sediment fluxes; and (4) Clarify the mechanism of the fractionation.

Appendix
(see pp. 256–257)

References

Arnorsson, S. and N. Oskarsson (2007): Molybdenum and tungsten in volcanic rocks and in surface and <100°C ground waters in Iceland. *Geochim. Cosmochim. Acta*, **71**, 284–304.

Boswell, S. M. and H. Elderfield (1988): The determination of zirconium and hafnium in natural waters by isotope dilution Mass Spectrometry. *Mar. Chem.*, **25**, 197–209.

Collier, R. W. (1985): Molybdenum in the Northeast Pacific Ocean. *Limnol. Oceanogr.*, **30**, 1351–1354.

Emery, W. J. (2001): Water types and water masses. p. 3179–3187. In *Encyclopedia of Ocean Sciences*, Vol. 4, ed. by J. H. Steele, S. A. Thorpe and K. K. Turekian, Academic Press, San Diego.

Ezoe, M., T. Ishita, M. Kinugasa, X. Lai, K. Norisuye and Y. Sohrin (2004): Distribution of dissolved and acid-dissolvable bioactive trace metals in the North Pacific Ocean. *Geochem. J.*, **38**, 535–550.

Firdaus, M. L., K. Norisuye, T. Sato, S. Urushihara, Y. Nakagawa, S. Umetani and Y. Sohrin (2007): Preconcentration of Zr, Hf, Nb, Ta and W in seawater using solid-phase extraction on TSK-8-hydroxyquinoline resin and determination by inductively coupled plasma-mass spectrometry. *Anal. Chim. Acta*, **583**, 296–302.

Gaillardet, J., J. Viers and B. Dupre (2005): Trace elements in river waters. p. 225–272. In *Treatise on Geochemistry*, Vol. 3, ed. by H. D. Holland and K. K. Turekian, Elsevier, Amsterdam.

Godfrey, L. V., W. M. White and V. J. M. Salters (1996): Dissolved zirconium and hafnium distributions across a shelf break in the northeastern Atlantic Ocean. *Geochim. Cosmochim. Acta*, **60**, 3995–4006.

Jochum, K. P., M. Seufert, B. Spettel and H. Palme (1986): The solar-system abundances of Nb, Ta and Y, and the relative abundances of refractory lithopile elements in differentiated planetary bodies. *Geochim. Cosmochim. Acta*, **50**, 1173–1183.

Johnson, K. S., R. M. Gordon and K. H. Coale (1997): What controls dissolved iron concentrations in the world ocean? *Mar. Chem.*, **57**, 137–161.

Li, Y.-H. (2000): *A Compendium of Geochemistry*. Princeton University Press, Princeton, 475 pp.

McKelvey, B. A. and K. J. Orians (1993): Dissolved zirconium in the north Pacific Ocean. *Geochim. Cosmochim. Acta*, **57**, 3801–3805.

McKelvey, B. A. and K. J. Orians (1998): The determination of dissolved zirconium and hafnium from seawater using isotope dilution inductively coupled plasma mass spectrometry. *Mar. Chem.*, **60**, 245–255.

Mito, S., Y. Sohrin, K. Norisuye, M. Matsui, H. Hasegawa, M. Maruo, M. Tsuchiya and M. Kawashima (2004): The budget of dissolved trace metals in Lake Biwa, Japan. *Limnol.*, **5**, 7–16.

Morford, J. L. and S. Emerson (1999): The geochemistry of redox sensitive trace metals in sediments. *Geochim. Cosmochim. Acta*, **63**, 1735–1750.

Nozaki, Y. (2001): Rare earth elements and their isotopes in the ocean. p. 2354–2365. In *Encyclopedia of Ocean Sciences*, Vol. 4, ed. by J. H. Steele, S. A. Thorpe and K. K. Turekian, Academic Press, San Diego.

Nozaki, Y., J. Zhang and H. Amakawa (1997): The fractionation between Y and Ho in the marine environment. *Earth Planet. Sci. Lett.*, **148**, 329–340.

Orians, K. J. and C. L. Merrin (2001): Refractory metals. p. 2387–2399. In *Encyclopedia of Ocean Sciences*, Vol. 4, ed. by J. H. Steele, S. A. Thorpe and K. K. Turekian, Academic Press, San Diego.

Park, K. H., D. Mohapatra and B. R. Reddy (2006): Selective recovery of molybdenum from spent HDS catalyst using oxidative soda ash leach/carbon adsorption method. *J. Hazard. Mat.*, **138**, 311–316.

Qiu, B. (2001): Kuroshio and Oyashio currents. p. 1413–1426. In *Encyclopedia of Ocean Sciences.*, Vol. 3, ed. by J. H. Steele, S. A. Thorpe and K. K. Turekian, Academic Press, San Diego.

Rudnick, R. L. and S. Gao (2005): The crust. p. 1–64. In *Treatise on Geochemistry*, Vol. 3, ed. by H. D. Holland and K. K. Turekian, Elsevier, Amsterdam.

Schlitzer, R. (2007): Ocean Data View (http://odv.awi.de).

Sohrin, Y., K. Isshiki, T. Kuwamoto and E. Nakayama (1987): Tungsten in North Pacific Waters. *Mar. Chem.*, **22**, 95–103.

Sohrin, Y., K. Isshiki, E. Nakayama, S. Kihara and M. Matsui (1989): Simultaneous determination of tungsten and molybdenum in sea water by catalytic current polarography after preconcentration on a resin column. *Anal. Chim. Acta*, **218**, 25–35.

Sohrin, Y., Y. Fujishima, K. Ueda, S. Akiyama, K. Mori, H. Hasegawa and M. Matsui (1998): Dissolved niobium and tantalum in the North Pacific. *Geophys. Res. Lett.*, **25**, 999–1002.

Sohrin, Y., M. Matsui and E. Nakayama (1999): Contrasting behavior of tungsten and molybdenum in the Okinawa Trough, the East China Sea and the Yellow Sea. *Geochim. Cosmochim. Acta*, **63**, 3457–3466.

Tatebe, H. and I. Yasuda (2004): Oyashio southward intrusion and cross-gyre transport related to diapycnal upwelling in the Okhotsk Sea. *J. Phys. Oceanogr.*, **34**, 2327–2341.

Turner, D. R., M. Whitfield and A. G. Dickso (1981): The equilibrium speciation of dissolved components in freshwater and seawater at 25°C and 1 atm pressure. *Geochim. Cosmochim. Acta*, **45**, 855–881.

Appendix. Dissolved and acid-dissolvable trace metals in the western North Pacific Ocean during MR05-K01.

Depth (m)	T (°C)	Salinity	Zr		Hf		Nb		Ta		Mo		W	
			D	AD	D	AD	D	AD	D	AD	D	AD	D	AD
St. K1														
10.0	2.255	33.226	42	50	0.21	0.25	4.7	5.9	0.12	0.14	97	97	41	42
30.8	2.257	33.227	44	50	0.22	0.27	5.1	6.1	0.14	0.16	103	100	46	43
51.7	2.258	33.228	39	47	0.25	0.29	4.8	6.5	0.11	0.13	105	105	47	51
76.0	2.241	33.230	45	53	0.23	0.27	5	6.1	0.15	0.16	99	100	49	43
101.5	2.269	33.242	40	50	0.21	0.24	4.7	6.2	0.12	0.14	97	99	50	47
126.7	3.716	33.840	45	55	0.25	0.26	4.9	5.9	0.15	0.16	102	97	50	50
150.7	3.708	33.884	55	63	0.27	0.29	5.1	5.7	0.13	0.15	98	103	45	43
200.2	3.741	33.979	50	61	0.24	0.26	5	5.9	0.16	0.18	99	105	42	42
251.0	3.656	34.048	60	69	0.23	0.24	5.3	6.2	0.14	0.16	100	100	43	50
301.0	3.645	34.108	62	73	0.25	0.28	5.6	5.7	0.17	0.17	100	98	50	49
400.8	3.461	34.194	65	72	0.25	0.25	5.5	5.9	0.14	0.15	103	102	49	50
499.8	3.297	34.255	73	79	0.27	0.29	5.5	5.8	0.13	0.14	105	99	41	45
600.7	3.138	34.299	80	88	0.27	0.31	5.6	5.8	0.13	0.15	98	101	43	47
800.5	2.847	34.375	75	89	0.25	0.29	5.4	6	0.14	0.16	97	99	47	47
1001.4	2.556	34.443	102	115	0.38	0.4	5.7	6	0.17	0.18	99	98	49	46
1003.3	2.554	34.443	120	132	0.36	0.41	5.9	6.4	0.18	0.19	101	97	50	48
1500.7	2.039	34.557	126	132	0.39	0.41	6.1	6.2	0.16	0.17	102	105	45	49
2000.1	1.763	34.614	155	159	0.41	0.42	6.3	6.4	0.17	0.18	99	104	47	42
2500.3	1.602	34.648	175	185	0.5	0.57	6	6.1	0.18	0.2	100	102	42	43
3001.5	1.515	34.666	170	192	0.52	0.61	6.2	6.5	0.19	0.2	98	97	48	44
3500.3	1.466	34.678	209	245	0.6	0.71	6.3	6.6	0.18	0.21	105	104	50	45
4001.8	1.463	34.682	200	241	0.65	0.81	6.1	6.8	0.2	0.22	101	105	49	44
4500.8	1.483	34.688	228	302	0.79	0.99	6.2	7	0.22	0.26	98	105	42	47
4764.8	1.503	34.692	265	349	0.82	1.1	6.9	8.4	0.29	0.35	99	105	50	50
St. K2														
11.1	1.469	33.056	40	49	0.2	0.25	5	6.2	0.11	0.13	100	101	40	45
30.3	1.462	33.056	42	48	0.21	0.25	4.7	5.9	0.12	0.14	97	97	48	40
50.9	1.463	33.056	45	55	0.2	0.25	4.8	6.6	0.1	0.12	100	99	41	40
75.5	1.469	33.056	41	47	0.22	0.25	4.9	6.1	0.09	0.1	99	100	49	45
100.0	1.469	33.058	40	47	0.23	0.29	5.1	6.2	0.1	0.11	101	103	43	42
125.3	2.847	33.597	47	57	0.24	0.3	5.2	6.5	0.11	0.11	102	104	45	48
150.3	3.268	33.759	50	60	0.25	0.3	5.1	5.9	0.12	0.14	99	99	48	49
199.7	3.474	33.892	59	74	0.27	0.31	4.8	5.5	0.1	0.11	97	103	50	47
249.0	3.525	33.983	62	75	0.28	0.31	5.2	5.7	0.13	0.15	100	101	47	47
301.1	3.472	34.049	78	95	0.27	0.32	5.3	5.8	0.15	0.16	98	102	44	46
402.0	3.358	34.157	82	92	0.29	0.31	5.5	6.3	0.14	0.15	105	98	50	48
499.2	3.216	34.226	89	100	0.3	0.35	5.6	5.9	0.12	0.14	104	98	40	45
600.6	3.066	34.292	83	110	0.31	0.36	5.2	6	0.14	0.16	101	100	48	51
799.8	2.762	34.383	110	121	0.37	0.39	5.4	5.5	0.15	0.17	102	99	47	43
1000.3	2.468	34.449	115	133	0.35	0.4	5.7	6.3	0.18	0.19	98	98	48	45
1500.0	2.018	34.561	128	139	0.37	0.39	5.9	6	0.19	0.2	97	103	45	48
2001.0	1.750	34.621	130	139	0.33	0.35	6.5	6.5	0.17	0.19	99	104	44	49
2502.0	1.592	34.652	140	159	0.35	0.4	6.2	6.3	0.16	0.18	103	104	46	50
2999.0	1.503	34.670	172	181	0.49	0.52	6.2	6.5	0.2	0.23	97	99	45	47
3500.0	1.451	34.687	179	190	0.56	0.59	6.3	6.7	0.21	0.23	99	97	45	49
4000.2	1.451	34.687	200	224	0.62	0.71	6.5	7	0.23	0.24	104	98	50	46
4500.7	1.476	34.691	245	285	0.76	0.9	7.1	7.5	0.24	0.27	99	104	45	48
4999.6	1.524	34.692	249	300	0.89	1.1	7	7.7	0.22	0.27	101	99	46	49
5133.3	1.537	34.693	275	352	0.95	1.2	7.2	8.3	0.27	0.33	102	104	47	51

Depth (m)	T (°C)	Salinity	Zr		Hf		Nb		Ta		Mo		W	
			D	AD	D	AD	D	AD	D	AD	D	AD	D	AD
St. KNOT														
10.7	2.184	33.160	51		0.19		4.6		0.1		100		43	
30.8	2.184	33.160	50		0.2		4.5		0.1		99		40	
49.6	2.185	33.161	51		0.25		5.7		0.12		101		47	
74.0	2.185	33.161	49		0.27		4.2		0.11		105		50	
101.7	2.193	33.162	48		0.23		4.7		0.12		97		49	
125.9	2.341	33.189	48		0.24		4.1		0.13		98		48	
151.2	2.838	33.416	53		0.27		5.4		0.12		100		40	
200.6	2.637	33.580	49		0.26		5.9		0.1		99		41	
249.7	2.881	33.714	50		0.23		5.6		0.11		102		42	
300.6	3.124	33.858	52		0.25		5.8		0.13		103		46	
400.7	3.704	34.074	55		0.25		6		0.12		104		49	
501.1	3.610	34.168	59		0.27		6.1		0.14		99		48	
601.0	3.278	34.208	75		0.23		5.4		0.15		103		44	
800.7	2.931	34.338	79		0.25		6.2		0.14		105		46	
1000.5	2.696	34.424	85		0.27		6.4		0.17		97		50	
1500.0	2.181	34.530	117		0.39		6.2		0.15		99		40	
2002.0	1.868	34.604	128		0.35		6.5		0.16		98		45	
2501.0	1.663	34.643	132		0.34		6.7		0.17		99		41	
3001.0	1.540	34.666	168		0.46		6.2		0.16		102		49	
3501.0	1.480	34.678	182		0.45		6.5		0.17		102		48	
4000.3	1.463	34.686	225		0.68		6.4		0.19		97		45	
4501.2	1.480	34.690	232		0.69		6.5		0.17		105		50	
5001.1	1.528	34.692	267		0.81		6.2		0.2		103		49	
5263.8	1.559	34.692	269		0.92		6.7		0.21		100		50	
St. 35N														
10.8	13.702	34.421	31	37	0.14	0.17	4	4.7	0.08	0.09	98	100	40	45
30.1	13.676	34.417	34	39	0.14	0.16	4.2	5.2	0.09	0.1	102	105	45	40
51.3	13.658	34.413	35	42	0.15	0.18	4.5	5.6	0.11	0.12	104	105	42	45
76.2	13.388	34.361	31	38	0.17	0.19	5.1	5.9	0.08	0.08	97	101	48	42
100.9	13.235	34.332	37	45	0.19	0.21	4.3	5.2	0.1	0.11	101	98	42	43
126.6	13.028	34.323	32	38	0.18	0.21	4.5	5.4	0.12	0.14	100	99	44	50
149.7	12.773	34.327	33	40	0.16	0.19	5.9	6.3	0.1	0.11	98	102	43	46
201.1	10.498	34.193	39	46	0.17	0.2	4.2	5	0.11	0.12	97	103	43	45
251.4	7.934	34.029	47	54	0.2	0.21	4.8	5.7	0.14	0.16	104	104	47	44
300.6	6.498	33.938	40	48	0.25	0.27	5	5.4	0.14	0.15	97	98	43	45
401.7	5.089	33.974	49	54	0.23	0.26	4.4	5.7	0.14	0.16	103	97	48	50
499.8	4.579	34.084	45	51	0.23	0.27	5.3	5.7	0.16	0.17	104	101	40	43
600.9	3.973	34.153	50	54	0.23	0.25	5.2	5.8	0.15	0.16	98	102	43	46
801.0	3.553	34.338	62	68	0.25	0.26	5.4	6	0.14	0.16	100	97	49	46
1000.5	3.001	34.409	81	87	0.27	0.3	5.7	5.9	0.15	0.16	105	100	48	45
1501.6	2.237	34.540	97	102	0.35	0.37	5.8	6.2	0.17	0.19	100	100	45	46
2001.4	1.839	34.613	121	142	0.35	0.41	5.5	5.7	0.15	0.17	98	105	44	48
2502.2	1.630	34.649	141	165	0.4	0.45	6.7	6.8	0.16	0.17	104	104	47	45
3002.1	1.496	34.671	146	189	0.42	0.53	6	6.4	0.19	0.21	100	100	45	46
3499.2	1.452	34.681	185	215	0.57	0.69	5.7	6.5	0.19	0.22	99	103	47	45
4001.4	1.446	34.687	243	291	0.62	0.8	6.3	7	0.2	0.22	103	99	50	48
4500.1	1.452	34.693	262	334	0.79	1	6.7	7.9	0.25	0.3	101	104	50	46

Notes:
Concentrations in pmol kg^{-1} except for Mo in nmol kg^{-1}.
Temperatures represent the observed temperature.